crystals

MDPI

Article

# Separating NaCl and $AlCl_3 \cdot 6H_2O$ Crystals from Acidic Solution Assisted by the Non-Equilibrium Phase Diagram of $AlCl_3$-NaCl-$H_2O$(-HCl) Salt-Water System at 353.15 K

**Huaigang Cheng [1], Jianwei Zhang [1], Huibin Lv [1], Yanxia Guo [1], Wenting Cheng [1], Jing Zhao [2] and Fangqin Cheng [1,*]**

[1] Institute of Resources and Environmental Engineering, State Environment Protection Key Laboratory of Efficient Utilization of Coal Waste Resources, Shanxi University, Taiyuan 030006, China; chenghg@sxu.edu.cn (H.C.); zjw20162400@163.com (J.Z.); david.ch@msn.cn (H.L.); experiments@126.com (Y.G.); wtcheng@sxu.edu.cn (W.C.)

[2] College of Chemical Engineering, Qinghai University, Xining 810016, China; sxzj1112@163.com

* Correspondence: cfangqin@sxu.edu.cn; Tel./Fax: +86-351-7018553

Academic Editor: Lan Xiang
Received: 30 June 2017; Accepted: 2 August 2017; Published: 4 August 2017

**Abstract:** Extracting $AlCl_3 \cdot 6H_2O$ from acid leaching solution through crystallization is one of the key processes to extracting aluminum from fly ash, coal gangue and other industrial solid wastes. However, the obtained products usually have low purity and a key problem is the lack of accurate data for phase equilibrium. This paper presented the non-equilibrium phase diagrams of $AlCl_3$-NaCl-$H_2O$ (HCl) salt-water systems under continuous heating and evaporation conditions, which were the main components of the acid leaching solution obtained through a sodium-assisted activation hydrochloric acid leaching process. The ternary system was of a simple eutonic type under different acidities. There were three crystalline regions; the crystalline regions of $AlCl_3 \cdot 6H_2O$, NaCl and the mixture $AlCl_3 \cdot 6H_2O$/NaCl, respectively. The phase diagram was used to optimize the crystallization process of $AlCl_3 \cdot 6H_2O$ and NaCl. A process was designed to evaporate and remove NaCl at the first stage of the evaporation process, and then continue to evaporate and crystallize $AlCl_3 \cdot 6H_2O$ after solid-liquid separation. The purities of the final salt products were 99.12% for NaCl and up to 97.35% for $AlCl_3 \cdot 6H_2O$, respectively.

**Keywords:** crystallization; phase diagram; high purity; $AlCl_3 \cdot 6H_2O$; NaCl

## 1. Introduction

Activation-leaching-crystallization is one of the key methods for extracting $AlCl_3 \cdot 6H_2O$ from coal fly ash [1], which is viewed as the bulk of industrial waste and is one of the most complex anthropogenic materials [2]. However, a large amount of NaCl is usually precipitated with the crystallization of $AlCl_3 \cdot 6H_2O$ as a result of the presence of a large number of sodium ions in the leaching solution. Since the solubilities of NaCl and $AlCl_3 \cdot 6H_2O$ are so high, they cannot be easily separated from each other. Therefore, separating NaCl from $AlCl_3 \cdot 6H_2O$ during the crystallization process is one of the key issues for making the process more feasible in the industry.

The crystallization method is a good option to extract $AlCl_3$ if the salt water system is relatively pure [3]. In general, the crystallization method has the widest application for salt separation from salt-water systems, including cooling crystallization, evaporation crystallization, salting-out crystallization, reaction crystallization and other methods [4]. For aluminum chloride, both salting out and evaporation are common crystallization methods. For instance, gaseous or liquid HCl is

usually added into the acid-leaching solution of aluminum-bearing minerals so that the solubility of $AlCl_3 \cdot 6H_2O$ is reduced for crystallization [5]. The solubility of $AlCl_3 \cdot 6H_2O$ can also be reduced by adding $FeCl_2$ into the Fe-Al-Mg-Ca-K-Cl-$H_2O$ system [6]. Evaporative crystallization is a more direct way, and refers to the method of removing some solvent through evaporation and getting precipitated crystals. The crystals usually need to be evaporated under negative pressure. However, no matter which method is used, it is not easy to separate NaCl and $AlCl_3$, due to their similar solubility at different temperatures. It should be noted that some similar studies have provided valuable information, suggesting that the separation of NaCl from $AlCl_3$ is feasible. For example, for the extraction of elements from acid leaching solution, some researchers have investigated the separation problems of $AlCl_3$, $FeCl_3$ and $CaCl_2$. All of these salts are soluble, and their solubility is similar to that of NaCl and $AlCl_3$. The phase diagrams [7,8] of the $AlCl_3$-$FeCl_3$-$H_2O$, $AlCl_3$-$CaCl_2$-$H_2O$ and $FeCl_3$-$CaCl_2$-$H_2O$ systems at 298.15 K were drawn, and then the evaporation process was optimized to achieve the separation of different components. Researchers studied the crystallization separation of crystalline $AlCl_3$ from fly ash with rich calcium impurities and mainly examined the phase diagrams of binary $AlCl_3$-$H_2O$ systems and ternary $AlCl_3$-$CaCl_2$-$H_2O$ systems within a temperature range of 278.15–363.15 K [7], which are very similar to the separation of NaCl from $AlCl_3$, meaning that there is the possibility of separating the two salts if there is a phase diagram.

References [9,10] reported the phase diagram of neutral $AlCl_3$-NaCl-$H_2O$ systems, which can provide a lot of information about the separation strategy between $AlCl_3$ and NaCl. For acidic leaching solutions, more solubility data of salts are necessary. Phase diagrams are undoubtedly one of the important topics in industrial crystallization [11]. Besides that, there is still a problem to which sufficient attention needs to be given; that of the non-equilibrium feature [12] of salt water systems during the industrial evaporation process. Forced evaporation is generally used in practical production, and the operation temperature is usually set at 353.15–368.15 K. There is a dynamic balance between continuous heating and evaporation in the practical process, and thus the phase diagram is different from that in an equilibrium status. As a result, a non-equilibrium phase diagram needs to be drawn if the separation between $AlCl_3$ and NaCl is to be optimized.

With regard to the non-equilibrium phase diagram data for the system in acidic conditions, the relevant research of the non-equilibrium phase diagram of the $AlCl_3$-NaCl-$H_2O$ (-HCl) salt-water system is carried out. After studying the phase diagram of the mixed system, the law of salt precipitation can be analyzed and then the technological process can be optimized to prepare pure $AlCl_3 \cdot 6H_2O$ and NaCl.

## 2. Materials and Methods

The non-equilibrium phase diagram of $AlCl_3$-NaCl-$H_2O$ salt-water system under acidic conditions was drawn. In a 1000 mL glass beaker placed in the constant temperature water bath, analytically pure $AlCl_3 \cdot 6H_2O$ (Tianjin Bodi Chemical Co., Ltd., Tianjin, China) was mixed with different concentrations of HCl (Shanxi Huihongyuan Chemical Co., Ltd., Taiyuan, China) solution at a temperature of 353.15 K and analytically pure NaCl (Tianjin Bodi Chemical Co., Ltd., Tianjin, China) was gradually added. Then, the beaker was tightly sealed using a plastic film. After 8 hours, the two salts reached equilibrium state, and the film was loosened so that the vapors could be slowly released at atmospheric pressure, and the heating-evaporation could be simultaneously maintained for about 1 hour, when the liquid phase was used to simulate the non-equilibrium conditions of evaporation of the leaching solution in an open system. The solution was then sampled and analyzed, and a series of solubility data was obtained. In the same way, a set of reverse experiments was carried out when the co-saturation phenomenon of the acidic solution of $AlCl_3$ and NaCl has occurred, i.e., NaCl was first dissolved in HCl solution followed by the addition of $AlCl_3 \cdot 6H_2O$.

The evaporation and precipitation features of the leaching solution were investigated. Firstly, an acidic solution containing 7.16 wt% $AlCl_3$ and 2.30 wt% NaCl, which is similar to the leaching solution in practice, was theoretically analyzed for the crystallization law of salts combined with the phase

diagram. Secondly, based on the typical components of the acid leaching solution of coal waste [5], analytically pure $AlCl_3 \cdot 6H_2O$, NaCl, $FeCl_3 \cdot 6H_2O$ (Tianjin Bodi Chemical Co., Ltd., Tianjin, China), $CaCl_2$ (Tianjin Bodi Chemical Co., Ltd., Tianjin, China) salts and HCl solutions were used to prepare the modeled leaching solution. The modeled solution contained 7.50 wt% $AlCl_3$, 4.89% NaCl, 1.75 wt% $FeCl_3$ and 2.26 wt% $CaCl_2$, which was evaporated to obtain high-purity NaCl and $AlCl_3 \cdot 6H_2O$ crystals guided by the calculation of phase diagram. In the preparation of the above solutions, the prepared solution was stirred for 12 h and kept standing for 12 h, respectively. Then a filtration with a pore size of 2.5 μm was carried out. The filtrate was put in a constant-temperature water bath for evaporation and crystallization. The obtained salt was separated and analyzed.

The precipitation ratio was used to describe the precipitated salt in comparison to the total salt dissolved in the feed solution, with the evaporation ratio referring to weight of the evaporated water compared to the feed solution in weight. The ion contents of liquid and solid phases were determined by inductively coupled plasma emission spectrometry, and then the purity of the salts was determined by the ion contents, which were finally converted to the mass contents of $AlCl_3 \cdot 6H_2O$ and NaCl.

## 3. Results and Discussion

### *3.1. The Phase Diagram of the $AlCl_3$-NaCl-$H_2O$ System*

The phase diagram of the $AlCl_3$-NaCl-$H_2O$ salt-water system under different $H^+$ concentrations is shown in Figure 1. Since the temperature of the acid leaching solution of fly ash is generally around 353.15 K in practical processes, there is no diagram drawn in ambient temperature. It can be seen that the phase diagram of the ternary system is of a simple eutonic type under different acidities, i.e., the system has no double salt or solid solution. As a comparison, some of the data of refereces [9,13] are included in Figure 1.

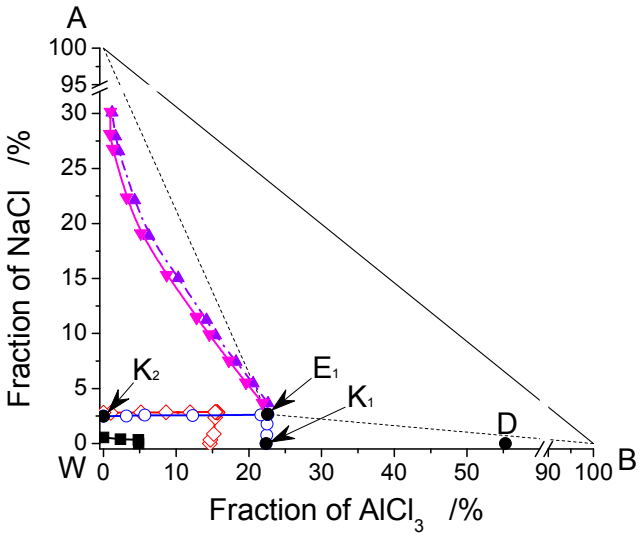


**Figure 1.** The phase diagram of $AlCl_3$-NaCl-$H_2O$ system. A—NaCl, B—$AlCl_3$, W—(HCl+$H_2O$), D—$AlCl_3 \cdot 6H_2O$; ○—$H^+$ = 1.3 mol/L at 353.15 K (this work), ◊—$H^+$ = 4.0 mol/L at 353.15 K (this work); ▲—Aqueous solution at approximate 330 K [9], ▼—Aqueous solution at approximate 298 K [9], ■—$H^+$ = 7.67 mol/L at 298.15 K [13].

The phase diagram consists of three solid phase crystalline regions, two solubility univariate curves and one co-saturated point. The points A, B and W represent the solid phase NaCl, $AlCl_3$ and the liquid phase, respectively. Besides those, there is another solid phase, i.e., the point D, representing $AlCl_3 \cdot 6H_2O$. Taking the phase diagram of the system with 1.3 mol/L in $H^+$ concentration as an example, there are three crystalline regions. The areas $BE_1K_1$ and $AE_1K_2$ are the crystalline regions of $AlCl_3$ and

NaCl, respectively, and $AE_1B$ is the co-crystalline region of $AlCl_3$ and NaCl. The curve $K_2E_1$ represents the solubility of NaCl, and the curve $K_1E_1$ shows that of $AlCl_3$. The point $E_1$ is the intersection of the solubility curves, indicating the co-saturated state of the leaching solution. According to the rules of the phase diagram, the composition of the solution would not be changed when its position is at the point $E_1$ in Figure 1.

Moreover, it can be seen that the acid concentration has a great impact on solubility, but the solubility curves are similar in trend under different acid concentrations. The solubility of the two salts is very low under hydrochloric acid conditions due to the homoion effect of $Cl^-$. In general, the increase in temperature helps the salts to be dissolved more easily, and the increase in acidity makes the salts dissolve less. For the $AlCl_3$-NaCl-$H_2O$ (-HCl) salt-water system, the effect of temperature on the solubility is not obvious, but the inhibition effect of acidity is very great. For example, the research [9] showed that the solubility of $AlCl_3$ in aqueous solutions increased from 31.16% (3.39 mol/kg in molality) to 31.53% (3.45 mol/kg) in mass percent when the temperature rose from 298.3 K to 338.1 K, for which increase of the solubility was not significant; the solubility of $AlCl_3$ increased from 30.15% (3.26 mol/kg) to 31.30% (3.44 mol/kg) in the aqueous solution containing 0.53–0.56% (0.134–0.138 mol/kg) NaCl in the same range of temperature. Similarly, when the concentration of $AlCl_3$ was about 30.47–30.61% (3.30–3.33 mol/kg), the solubility of NaCl increased from 0.37% (0.092 mol/kg) to 0.84% (0.21 mol/kg) when the temperature rose from 298.1 K to 322.9 K [9]. All of the increases in solubility were relatively small; thus, it could be considered that the solubility of salts did not change much at different temperatures in the $AlCl_3$-NaCl-$H_2O$ system. In contrast, the effect of acidity on the solubility in the system was more significant. For instance, Figure 1 shows that the solubility of $AlCl_3$ only reaches 22.60%, although the temperature was higher, and thus the dissolution was easier enhance, where the value of solubility in acidic solutions was much lower than that under neutral conditions [9]. Furthermore, the stronger the acidity in Figure 1, the smaller the solubility of $AlCl_3$. Similarly, the research work [9] showed that the solubility of NaCl in aqueous solution was about 22.64% (5.252 mol/kg) when the concentration of $AlCl_3$ was about 3.67% (0.373 mol/kg), while the solubility of NaCl was only about 2.55 % ($H^+$ = 1.3M) to 2.80% ($H^+$ = 4.0M) under the acidic conditions in Figure 1. The NaCl solubility could only reach lower than 0.55% when the $H^+$ concentration reached 7.67 mol/L (28 wt% HCl) [13]. Obviously, these phenomena were caused by the strong inhibition of solubility by acidity. In addition, it should have to be noted that the solubility of NaCl unexpectedly increases when the acidity increases in Figure 1; presumably, this phenomenon could be due to the non-equilibrium evaporation state. Since the acidic solution was already in an unbalanced state for one hour at the time of sampling, the acidity drop caused by the volatilization of HCl and the convection of the liquid phase caused by heating might increase the solubility of NaCl, which made the salt solubility slightly disordered.

### *3.2. The Analysis of Crystallization Process Based on Phase Diagrams*

Figure 2 shows a part of the phase diagram of $AlCl_3$-NaCl-$H_2O$ system. Firstly, the process of evaporating crystals from the acid leaching solution is analyzed. As shown in Figure 2, the phase point M representing the feed solution in the phase diagram at 353.15 K is found. When the solution at point M is concentrated during the evaporation process, the system point moves away from the liquid point W due to loss of water until the solution begins to precipitate solid salt crystals. At this moment, the solid phase point is locked at point A of NaCl. When the evaporation continues, the liquid phase point moves from point M to point L, representing the saturated state of NaCl in the leaching solution and then to point $E_1$ along the saturation curve. Finally the solid phase, liquid phase and system points are located at points A, $E_1$ and $M_1$, respectively. In this process, the system point falls into the crystallization region of NaCl, and thus the solid NaCl first gets saturated and begins to precipitate out. The system includes two parts, i.e., the solid phase of NaCl and the solution that is saturated for NaCl. According to the lever law of the phase diagram, the precipitation amount of NaCl can be calculated by $M_1E_1/AE_1$. It can be seen that the ratio of $M_1E_1/AE_1$ increases along with the

evaporation process, indicating that the precipitation amount of NaCl is gradually increasing. The precipitation amount of NaCl reaches the maximum value when the system point reaches $M_1$ and the liquid phase point reaches $E_1$. Then, solid-liquid separation should be carried out to obtain the pure NaCl and the solution at point $E_1$. When the evaporation of solution $E_1$ continues, the liquid phase point is locked at point $E_1$ because it represents the co-saturated solution of NaCl and $AlCl_3$ and the degree of freedom is zero in the co-crystalline region of the two solid phases. The solid phase $AlCl_3{\cdot}6H_2O$ begins to precipitate, and the solid phase point appears at the point $S_1$, representing the mixture of NaCl and $AlCl_3{\cdot}6H_2O$, and then the system point gradually moves towards $S_1$ until the solution $E_1$ is evaporated to dryness. Finally, the liquid phase point disappears at point $E_1$ and the solid mixture at point $S_1$ is obtained. According to the coordinates of $E_1$, the obtained salt should comprise 6.15% NaCl and 93.85% $AlCl_3{\cdot}6H_2O$ in weight percent. Based on the phase diagram rules, 93.85% should be the upper limit of the purity of $AlCl_3{\cdot}6H_2O$ prepared by using the evaporation method. According to the lever rule of the phase diagram, about 40% of the water should be evaporated out of the feed leaching solution when the system point moves from M to L and then the solid NaCl begins to precipitate. Before the liquid phase point reaches $E_1$, it is in the single crystalline region of NaCl. At this time, the obtained salt should be pure NaCl; after a further 50% water is evaporated, the liquid phase point reaches point E and the mixed salts of NaCl and $AlCl_3{\cdot}6H_2O$ are gradually precipitated.

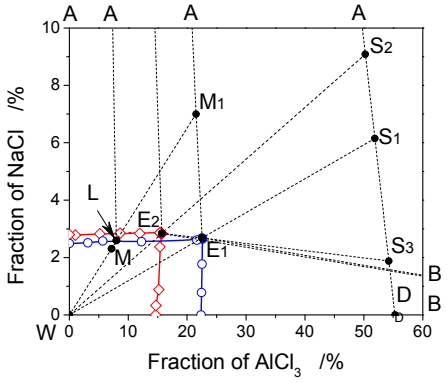


**Figure 2.** The part of the phase diagram of the NaCl-$AlCl_3$-$H_2O$ system at 353.15 K. A—NaCl, B—$AlCl_3$, W—(HCl+$H_2O$), D—$AlCl_3{\cdot}6H_2O$; ○—$H^+$ = 1.3 mol/L, ◊—$H^+$ = 4.0 mol/L.

Secondly, the acid-adding crystallization process of the leaching solution is analyzed. As shown in Figure 2, the concentrated hydrochloric acid should be added when the solution at point $E_1$ has been obtained. The solution at point $E_1$ immediately falls into the area of $AE_2B$, representing the co-precipitation region of NaCl and $AlCl_3{\cdot}6H_2O$ when $H^+$ reaches 4.0 mol/L in concentration, and the liquid and solid phase points appears at $E_2$ and $S_3$, respectively. The coordinates of $S_3$ show that the precipitated salt should be 1.88% NaCl and 98.12% $AlCl_3{\cdot}6H_2O$ in weight percent. The purity of $AlCl_3{\cdot}6H_2O$ is higher than that in the previous study [5]. However, calculated based on the lever rules of the phase diagram, the precipitated solid phase is less than about 0.18 times the weight of the whole solution at point $E_1$, and most of the $AlCl_3$ still exists in the solution at point $E_2$, leading to a low yield. If the solution at point $E_2$ is evaporated to dryness, the solid product at point $S_2$ shows an $AlCl_3{\cdot}6H_2O$ content of 90.91%. It should be noted that, similar to the analysis of Figure 1, there was a certain degree of disorder phenomenon in the non-equilibrium evaporation and acid-adding processes, which could make the quality of the final product lower than the expectations in Figure 2. However, in any case, the analysis process based on Figure 2 was generally predictive of the grade of the product. In general, pure salt crystals can be achieved using the method of acid addition, but a large consumption of acid may be necessary. For example, the crystallization process in the previous study [5] is similar to the process in Figure 2, suggesting that $AlCl_3{\cdot}6H_2O$ could reach 96.8% in purity when the HCl is about 7.40 mol/L (27.0%) in concentration [5], which is close to the theoretical expectation in Figure 2.

### *3.3. Optimization of Crystallization Process Based on Phase Diagram*

Figure 3 shows the precipitation ratio of solid salt when the acid leaching solution is evaporated at 1.3 mol/L in $H^+$ concentration. The precipitation ratio of NaCl was more than 90% when the evaporation ratio of the acid leaching solution reached about 78%, while the crystallization ratio of $AlCl_3 \cdot 6H_2O$ was only about 20%. After that, the precipitation ratio of $AlCl_3 \cdot 6H_2O$ was obviously accelerated. In Figure 3, $AlCl_3$ began to precipitate significantly after the NaCl content was reduced to a certain amount, which is in accordance with the analysis of Figure 2. However, there was a phenomenon that the $AlCl_3 \cdot 6H_2O$ was precipitated a little ahead of the prediction of Figure 2, which was assumed to be because $FeCl_3$ and $CaCl_2$ affected the phase transition of $AlCl_3 \cdot 6H_2O$. Since the precipitation sequence of NaCl and $AlCl_3 \cdot 6H_2O$ agreed basically with the theoretical analysis of Figure 2, the phase diagram can be considered reliable, and can be used to guide the separation of pure NaCl and $AlCl_3 \cdot 6H_2O$.

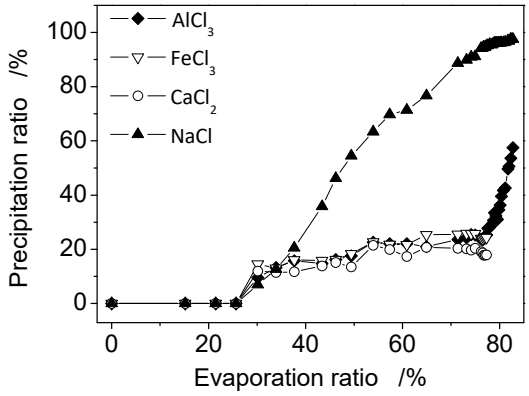


**Figure 3.** The precipitation sequence of crystal salts.

It is worth mentioning that the precipitation ratio for calcium chloride and iron chloride was approximately 20% when the leaching solution exhibited approximately an evaporation ratio of 23–78%. It is assumed that the high ion strength in the leaching solution greatly decreased the solubility of $FeCl_3$ and $CaCl_2$, resulting in their precipitation in advance. For instance, the data for the phase equilibrium of the $AlCl_3$-$CaCl_2$-$H_2O$ system [7] has provides an example; i.e., the solubility of $CaCl_2$ sharply fell from 59.52% (13.246 mol/kg) to 0 when the concentration of $AlCl_3$ rose from 0 to 32.52% (3.610 mol/kg) at 353.15 K. The $AlCl_3$-$FeCl_3$-$H_2O$ system [8] showed a similar phenomenon. This means that the solubility of $FeCl_3$ and $CaCl_2$ can be significantly reduced in the concentrated salt solution.

After considering the above theoretical analysis and experimental results, the technological processes described in Figure 2 were tested. The acid leaching solution of fly ash was used for the experiment to prepare salt crystals. Following crystallization and solid-liquid separation, the purity of the final salt products is shown in Table 1. It can be seen that the NaCl and $AlCl_3 \cdot 6H_2O$ reach 99.12% and 97.35% in purity, respectively, which is higher than the previous results [5]. However, it is important to note that, in the actual process experiment, when the temperature is high, the mixture of $AlCl_3 \cdot 6H_2O$ and NaCl derived from the separation may contain a large iron salt and calcium salt content. It is assumed that the iron-calcium impurities may be entrained when the precipitation of $AlCl_3 \cdot 6H_2O$ and NaCl occurs. Furthermore, fluid mechanics also have a great influence on the precipitation, which may affect the purity of salts in the practical production.

**Table 1.** The purities of precipitated salts.

| Salts | Contents (wt%) | | | | |
|---|---|---|---|---|---|
| | $AlCl_3 \cdot 6H_2O$ | | NaCl | | Impurities |
| | Experimental | Theoretical | Experimental | Theoretical | |
| NaCl | 0 | 0 | 99.12 | 100.00 | 0.88 |
| $AlCl_3 \cdot 6H_2O$ ($S_1$) | 90.06 | 93.85 | 5.20 | 6.15 | 4.74 |
| $AlCl_3 \cdot 6H_2O$ ($S_3$) | 97.35 | 98.12 | 1.32 | 1.88 | 1.33 |

## 4. Conclusions

The non-equilibrium phase diagram of $AlCl_3$-NaCl-$H_2O$ (-HCl) salt-water systems under continuous heating and evaporation conditions was investigated. The ternary system is of a simple co-saturated type under different acidity conditions, i.e., the system has no double salt or solid solution. The phase diagram consists of one co-saturated point, two solubility univariate curves and three solid phase crystalline regions of pure $AlCl_3 \cdot 6H_2O$, pure NaCl and mixed $AlCl_3 \cdot 6H_2O$/NaCl, respectively. Increasing the acidity will reduce the solubility of each salt. The phase diagram was used to analyze the crystallization process of $AlCl_3 \cdot 6H_2O$ and NaCl. The crystallization rule of the acid leaching solution at different acidities was analyzed theoretically and experimentally. Based on the phase diagrams, a procedure was designed to remove NaCl at the first stage of evaporation, and then continue to evaporate and crystallize $AlCl_3 \cdot 6H_2O$ after solid-liquid separation. The experimental results of this program were consistent with the prediction based on the phase diagram, and NaCl and $AlCl_3 \cdot 6H_2O$ with purities of 99.12% and up to 97.35%, respectively, were finally obtained.

**Acknowledgments:** This work was financially supported by National Natural Science Foundation of China (51674162), the Tri-Jin Scholars and Natural Science Foundation of Shanxi Province (201601D102058) and the Provincial Research Projects (2016JD06, 2016-HZ-803).

**Author Contributions:** Huaigang Cheng and Fangqin Cheng conceived and designed the experiments; the high-purity NaCl and $AlCl_3 \cdot 6H_2O$ crystals were separated from acidic solution by Jianwei Zhang, and the data of non-equilibrium phase diagram was obtained by Huibin Lv; the experimental platform and corresponding support were provided by Fangqin Cheng; Huaigang Cheng drew the phase diagram and analyzed the data with Yanxia Guo, Wenting Cheng and Jing Zhao; Huaigang Cheng wrote the paper.

**Conflicts of Interest:** The authors declare no conflict of interest.

## References

1. Sibanda, V.; Ndlovu, S.; Dombo, G.; Shemi, A.; Rampou, M. Towards the Utilization of Fly Ash as a Feedstock for Smelter Grade Alumina Production: A Review of the Developments. *J. Sustain. Metall.* **2016**, *2*, 167–184. [CrossRef]
2. Yao, Z.T.; Ji, X.S.; Sarker, P.K.; Tang, J.H.; Ge, L.Q.; Xia, M.S.; Xi, Y.Q. A comprehensive review on the applications of coal fly ash. *Earth-Sci. Rev.* **2015**, *141*, 105–121. [CrossRef]
3. Gong, J.B.; Wang, Y.; Du, S.C.; Dong, W.B.; Yu, B.; Wu, S.G.; Hou, J.; Wang, J.K. Industrial Crystallization in China. *Chem. Eng. Technol.* **2016**, *39*, 807–814. [CrossRef]
4. Lewis, A.; Seckler, M.; Kramer, H.; Van Rosmalen, G. *Industrial Crystallization: Fundamentals and Applications*, 1st ed.; Cambridge University Press: Cambridge, UK, 2015; pp. 4–13.
5. Guo, Y.; Lv, H.; Yang, X.; Cheng, F. $AlCl_3 \cdot 6H_2O$ recovery from the acid leaching liquor of coal gangue by using concentrated hydrochloric inpouring. *Sep. Purif. Technol.* **2015**, *151*, 177–183. [CrossRef]
6. Gao, W.C.; Li, Z.B. Solubility of $AlCl_3 \cdot 6H_2O$ in the Fe(II) plus Mg plus Ca plus K+Cl+$H_2O$ System and its salting-out crystallization with $FeCl_2$. *Ind. Eng. Chem. Res.* **2013**, *52*, 14282–14290. [CrossRef]
7. Wang, J.; Petit, C.; Zhang, X.; Cui, S. Phase Equilibrium Study of the $AlCl_3$-$CaCl_2$-$H_2O$ System for the Production of Aluminum Chloride Hexahydrate from Ca-Rich Flue Ash. *J. Chem. Eng. Data* **2016**, *61*, 359–369. [CrossRef]
8. Yuan, M.; Qiao, X.; Yu, J. Phase equilibria of $AlCl_3$ + $FeCl_3$ + $H_2O$, $AlCl_3$ + $CaCl_2$ + $H_2O$, and $FeCl_3$ + $CaCl_2$ + $H_2O$ at 298.15 K. *J. Chem. Eng. Data* **2016**, *61*, 1749–1755. [CrossRef]

9. Farelo, F.; Fernandes, C.; Avelino, A. Solubilities for Six Ternary Systems: NaCl+$NH_4Cl$+$H_2O$, KCl+$NH_4Cl$+$H_2O$, NaCl+LiCl+$H_2O$, KCl+LiCl+$H_2O$, NaCl+$AlCl_3$+$H_2O$, and KCl+$AlCl_3$+$H_2O$ at T=(298 to 333) K. *J. Chem. Eng. Data* **2005**, *50*, 1470–1477. [CrossRef]
10. Sarkarov, R.A.; Mironova, O.P. Solubility in the $AlCl_3$-LiCl-NaCl-$H_2O$ System. *Zh. Neorg. Khim.* **1990**, *35*, 280–282.
11. Ulrich, J.; Frohberg, P. Problems, potentials and future of industrial crystallization. *Front. Chem. Sci. Eng.* **2013**, *7*, 1–8. [CrossRef]
12. Zhou, H.; Chen, Y.; Kang, Q.; Zhang, J.; Zhang, H.; Yuan, J.; Sha, Z. Non-equilibrium State Salt-forming Phase Diagram: Utilization of Bittern Resource in High Efficiency. *Chin. J. Chem. Eng.* **2010**, *18*, 635–641. [CrossRef]
13. Skiba, G.S.; Sel'kina, Y.A. The NaCl-$AlCl_3$-HCl-$H_2O$ System at 25 °C. *Russ. J. Inorg. Chem.* **2016**, *61*, 1031–1034. [CrossRef]